

## Figure of Merit Optimization of the Event Selection Program for Data Analysis in the NOvA Far Detector

Benedectus Juwono\*  
*University of California, San Diego*

### Abstract:

The NuMI Off-axis  $\nu_e$  Appearance Experiment, designed to study the oscillation of neutrinos from one flavor to another, consists of two detectors placed off-axis from the main NuMI beamline: the near detector and the far detector. The data collected in the far detector, located approximately 810 km away from the Fermilab site, will be compared with the data collected in the near detector, located at Fermilab, to determine whether oscillation from  $\nu_\mu$  to  $\nu_e$  has occurred. As a result, it is vitally important to be able to distinguish signal ( $\nu_\mu \rightarrow \nu_e$ ) events from background ( $\nu_e$  contamination,  $\nu_\mu$  charged current,  $\nu_\mu$  neutral current) events in the far detector. The sensitivity of the experiment is characterized by the Figure of Merit (FoM) =  $\frac{\text{signal}}{\sqrt{\text{background}}}$ , which must be optimized.

## I. Introduction

Experiments in Neutrino Physics done in the past two decades have greatly advanced our understanding of neutrinos, and provided us with the knowledge that the three flavors of neutrinos ( $\nu_e$ ,  $\nu_\mu$ , and  $\nu_\tau$ ), each of which is associated with a lepton (e,  $\mu$ , and  $\tau$ , respectively), are a mixture of three neutrino mass states ( $\nu_1$ ,  $\nu_2$ , and  $\nu_3$ ) with specific masses ( $m_1$ ,  $m_2$ , and  $m_3$ ). The flavor eigenstates are related to the mass eigenstates by the equation

$$|\nu_\alpha\rangle = \sum_i U_{\alpha i} |\nu_i\rangle$$

where  $\nu_\alpha$  are the flavor eigenstates,  $\nu_i$  are the mass eigenstates, and  $U$  is the unitary lepton mixing matrix. The fact that the flavors are combinations of different mass-specific neutrino types allows for oscillation to occur from one flavor to another. The probability for such an oscillation to occur is given to the first order by

$$P(\nu_\mu \rightarrow \nu_e) = 0.5 \sin^2(2\theta_{13}) \sin^2\left(\frac{1.27 \Delta m_{13}^2 L}{E}\right)$$

where  $(\Delta m_{13})^2 \approx (\Delta m_{32})^2 = 0.0025 \text{ eV}^2$ , and  $L = 810 \text{ km}$ . The energy distribution  $E$  is given by

the NuMI medium energy beam, and  $\theta_{13}$  is the mixing angle parameter that is currently unknown, but CHOOZ and SuperK have provided a certain limit to this parameter. The mixing angle depends on the value of  $(\Delta m_{32})^2$ , and for the particular  $(\Delta m_{32})^2$  value used above, the limit is  $\sin^2(2\theta_{13}) < 0.14$ . NOvA hopes to measure  $\theta_{13}$ , determine the sign of  $(\Delta m_{32})^2$ , and possibly detect CP violation. Note that the oscillation probability above does not take into account matter, solar, and CP violation effects.

## II. Background and Procedure

The main idea used in this experiment is fairly simple. The NuMI beam will supply the flux of  $\nu_\mu$  that will then be sent to the near detector for prior measurements of  $\nu_e$  contaminations. The data collected in the near detector will determine, to a good accuracy, how much  $\nu_e$  is contaminating the  $\nu_\mu$  beam and how much background is produced by  $\nu_\mu$  CC and NC interactions. This is a fairly significant part of the procedure for the purpose of final data comparison with the far detector. From here, the  $\nu_\mu$  beam (with a small

---

\*Advisor: Peter J. Litchfield, *University of Minnesota*

fraction of  $\nu_e$  from contamination) will travel approximately 810 km, following the main beam-line path, and along the way to the far the detector, some of the  $\nu_\mu$  may (or may not) oscillate into  $\nu_e$ . The data collected in the far detector will be compared with the data collected in the near detector, and any significant discrepancy in the data readout of the two detectors can therefore be accounted for oscillation.

Neutrinos have a low probability of interacting with matter, and this is one fact that presents some difficulties to the experiment. This low-probability interaction will be compensated by sending  $6.5 \times 10^{20}$  proton on target per year from the Fermilab site. The amount of  $\nu_\mu$  produced in the initial process will be of the same order of magnitude. In the energy regime of 2 GeV, at which the oscillation probability peaks, four different processes may occur in the detector: Quasielastic (QE), Resonance, Coherent, and Deep Inelastic Scattering (DIS). These processes may be neutral-current (NC), which occurs via Z-boson exchange, or charged-current (CC), which occurs via W-boson exchange.

A QE process is one of the “cleanest” processes that may occur: the interaction between the neutrino and the nucleus results in, a nucleon and a charged lepton. For an NC event, hadrons and a neutrino are produced. A Resonant process produces a resonance, which then decays into pions, along with a neutron or a proton. In a Coherent process, the neutrino scatters off the nucleus entirely, producing a neutrino and a  $\pi^0$  for a NC event. A DIS process is typically messy, for it produces multiple pions.

Neutral pions produced in non-quasielastic processes may create showers that get misidentified as ones that are produced by electrons. This is very likely to occur in a NC Resonance or a NC DIS process, especially if the neutrino that initiates the interaction has a high enough energy to produce multiple  $\pi^0$ , which causes a “messy” event with several showers overlapping one another, or simply one  $\pi^0$  that has enough energy to shower and fake a  $\nu_e$  CC event. Due to these, it is vitally important to develop and optimize an event selection program that can distinguish between a fake (background)  $\nu_e$  CC event and a real (signal)  $\nu_e$  CC event.

### III. Event Selection Procedure

The signals and backgrounds for  $\nu_\mu \rightarrow \nu_e$  oscillations have been generated using the GEANT3 detector simulation and NEUGEN3

neutrino interaction generator for a five-year run, and then weighted accordingly to produce the correct distribution and number of events. After reconstruction (finding and fitting tracks) and calculation of various parameters associated with the tracks, the reconstruction program then assigns different particles to different tracks and calculates the interaction vertex. The reconstruction parameters that will be used to separate signal events from background events are then compiled as ntuples, which consist of the following variables:

- a. Total measured energy
- b. Pulse height asymmetry of the event
- c. Electromagnetic energy
- d. Energy in muon track
- e. Hadron energy
- f. Potential pion mass
- g. Backwards energy
- h. Energy in the back and transverse edge of the detector
- i. Number of planes with hits
- j. Average number of hits per plane
- k. Average pulse height per plane
- l. Fraction of total energy in the first-half of the planes
- m. Fraction of total energy assigned to electron
- n. Gap distance from the main vertex (or first hit)
- o. Number of gaps in front of and on a track
- p. RMS
- q. Curvature of fitted track

The process of separation between signals and backgrounds is done by first using a set of loose preliminary cuts, and then applying a maximum likelihood analysis to half of the surviving events. The maximum likelihood cut that maximizes the Figure of Merit (FoM) of this half of the generated events (the training set) can be determined from this analysis, and then applied to the other half of the surviving events. This is done because this maximum likelihood cut is determined using known information that is not available in the actual experiment. We assume that both halves of the data exhibit the same characteristics and thus applying the cut obtained from the training data to obtain the FoM of the other half will be close to simulating the actual experiment. The loose preliminary cuts applied to all of the generated data select only events that exhibit the following characteristics:

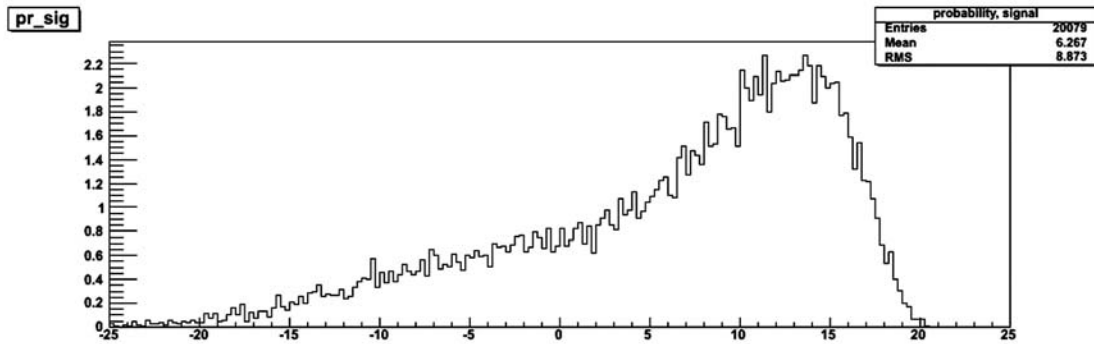


Figure 3.1

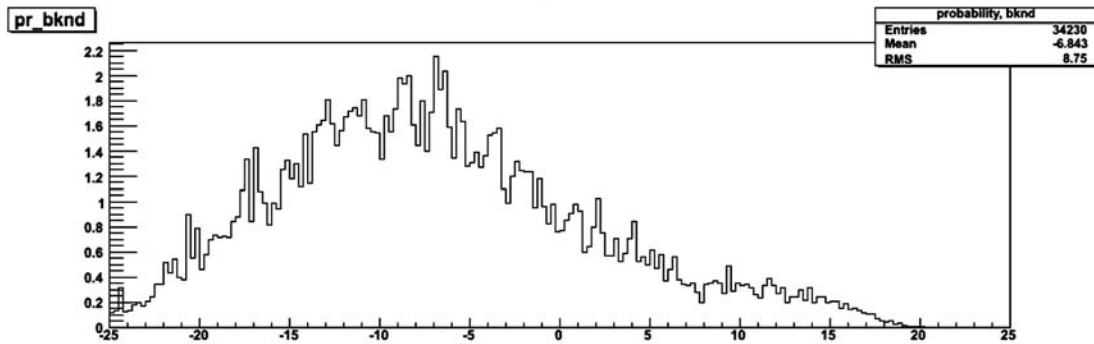


Figure 3.2

**Top:** The distribution of half of the generated signal events as a function of the total likelihood (in natural log).

**Bottom:** The distribution of half of the generated background events as a function of the total likelihood (also in natural log). These histograms show that when an event has a positive likelihood, it is more likely to be a signal event, and when it has a negative likelihood, it is more likely to be a background event. The maximum cutoff value obtained from this half of the data is  $L = 6.25$ .

1. A measured energy within 25% of the nominal-axis energy
2. No significant energy deposition near the detector edges
3. An electron candidate, which starts near the vertex and no gaps near the vertex
4. No  $\mu^-$  or  $\gamma$  in the event.

Half of the signal and background events that survive these preliminary cuts are then used to fill histograms based on different parameters. For each parameter, signal events will be filled into signal histograms, and background events will be filled into background histograms. These histograms are then normalized into probability histograms, such that the probability of an event, given a certain parameter value, to be a signal or a background can be determined by simply referring to the histogram for that particular parameter. The total likelihood of each event to be a signal or a background can then be determined by multiplying together the probabilities of all the

parameters associated with that particular event. For simplicity, natural logarithm scale is used for the total likelihood.

$$L = \prod p_i$$

$$\ln(L) = \ln(\prod p_i)$$

$$\ln(L) = \sum \ln(p_i)$$

where  $L$  is the total likelihood of an event, and  $p_i$  is the probability of parameter  $i$  of that particular event. From this point on, whenever likelihood is mentioned, we actually mean the natural logarithm of the likelihood.

The total likelihood of each event is then filled into two probability histograms: one for signal and one for background. Using these two histograms, the maximum likelihood cut for the training data can be determined. Figure 3.1 and 3.2 illustrate the probability plots of the total likelihoods of half of the events that have passed the preliminary cuts. The FoM of this half can be determined by counting the number of signal

Excluded Parameter	FoM
None	23.0
Total Energy	22.5
PH Fraction of $c$	23.1
Track Length	23.1
Avg PH in Front Planes	22.9
PH / Plane	23.0
Hits / Plane	22.8
Backwards Energy	22.5
Unused PH Fraction	23.6
Curvature	23.1
PH Asymmetry	22.8
No. of Gaps	23.2
Avg PH in First Half of Planes	23.4
RMS Compressed	23.1
Mass of Pion	22.8

Table 4.1

Variation of FoM obtained by excluding different parameters from calculating final total likelihood. The maximum FoM of 23.9 is obtained by excluding Unused PH Fraction, No. of Gaps, and Avg PH in the First Half of Planes. As seen from the table, these are the three parameters that increase the training FoM the most from what it is originally with all parameters included.

events and background events to the right of the bin where the two distribution curves intersect, taking the likelihood value associated with this bin as a lower cutoff value. Since this most likely will not give a maximum FoM, we then increase this cutoff value using an increment of one bin until we reach a bin that gives a maximum FoM. The likelihood value associated with this final bin will be the maximum likelihood cutoff value, which will then be applied to the probability plots of the other half of the data in order to simulate the actual experiment.

#### IV. Event Selection Program

The current event selection program whose performance is being tested and optimized is one by Professor Stanley Wojcicki (*Stanford University*). Using the analysis described above, and simulated signal and background events for a 25 kT detector, located 12 km off-axis, the program manages to obtain a maximum training FoM of 23.9, which corresponds to a maximum likelihood cutoff value of 6.25, and a FoM of 23.6 when that cutoff value is applied to the other half of the data.

This FoM is obtained by excluding the following parameters in filling the final signal and background probability plots:

- Unused fraction of pulse height
- Number of gaps
- Pulse height fraction in the first half of the plane

Including these parameters, or excluding any of the other ones, decreases the FoM obtained in the training analysis, although not by any significant amount. Table 4.1 illustrates how the training FoM varies as different parameters are excluded from the probability calculation.

The decrease in FoM when the three parameters above are included shows that there is still more background than signal events in the distribution histograms of these parameters, even after all the strict cuts are applied. This calls for further studies on the three parameters to determine whether it is possible to devise a way to re-define their loose and strict cuts such that more background events than signal are rejected. The histograms that represent the distribution of signal and background events for these parameters are shown in Figure 4.1, 4.2, and 4.3.

The process of eliminating each type of the background events done by this program is quite remarkable. In terms of separating  $\nu_\mu$  CC events

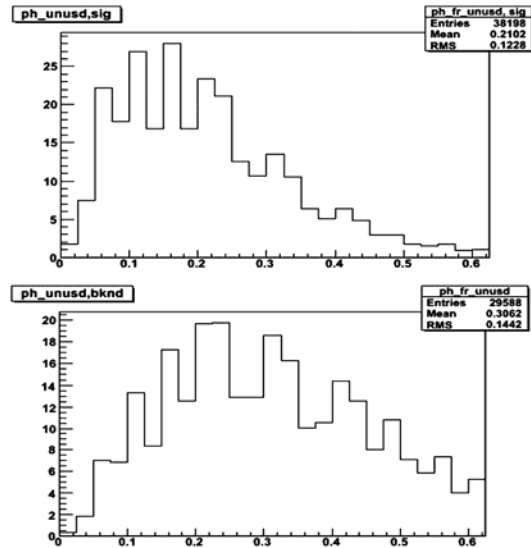


Figure 4.1

**Top:** Unused PH Fraction of signal events. **Bottom:** Unused PH Fraction of background events. The two distributions overlap each other almost entirely, making it hard to separate signal events from background.

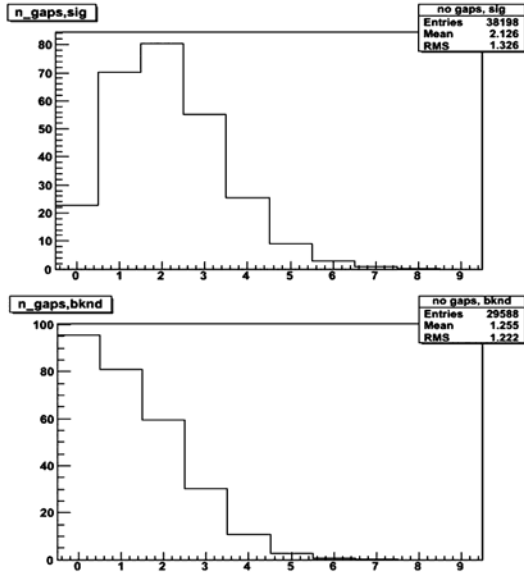


Figure 4.2

**Top:** Distribution of number of gaps on a track for signal events. **Bottom:** Distribution of number of gaps on a track for background events. The only distinguishing feature between the two distributions is that near zero, there are about three times more background events than signal. Other than that, however, they pretty much overlap.

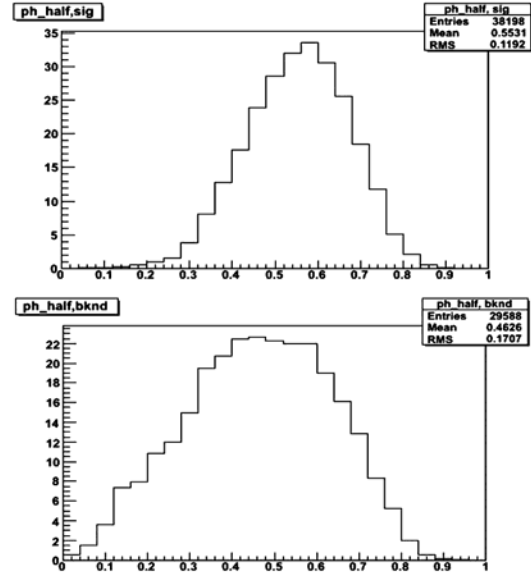


Figure 4.3

**Top:** Distribution of PH in the first half of planes for signal events. **Bottom:** Distribution of PH in the first half of the planes for background events. The two distributions look similar, but the background distribution is a little wider.

from  $\nu_e$  CC events, the program did extremely well. As seen in Table 4.2, the program manages to eliminate all but one of the  $\nu_\mu$  CC events generated. Even the loose cuts themselves manage to

narrow down the  $\nu_\mu$  CC events to about 6% the starting number. Figure 4.4 illustrates how well the separation between muon events and electron events is for one of the parameters.

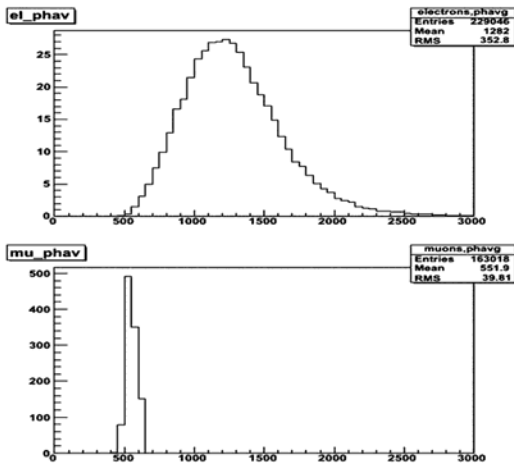


Figure 4.4

**Top:** Average pulse height distribution for electron events. **Bottom:** Average pulse height distribution for muon events. The two distributions are clearly distinct and an appropriate cutoff value can be determined to eliminate all muon events with only a small loss of electron events.

For  $\nu_\mu$  NC events, the loose cuts manage to cut down to about 6%, but a very small fraction (about 0.14%) of the initial events still manage to pass the maximum likelihood cuts. Although the fraction seems small enough to be negligible, it ends up being quite significant due to the large number of  $\nu_\mu$  NC events generated.

$\nu_e$  beam events still make up the most of the background events, however, since they are basically electron events and aside from the initial energy distribution, which is flat for  $\nu_e$  beam and peaked for  $\nu_e$  oscillation, there is little hope in being able to distinguish them from electron events initiated by  $\nu_\mu \rightarrow \nu_e$  oscillation. The loose cuts manage to narrow the beam events down to about 15%, and are then reduced further down to about 6% by the strict and maximum likelihood cuts.

Although a FoM of  $\sim 24$  is considered to be good, it is quite a concern that the event selection program only manages to keep less than 30% of the oscillation (signal) events. Table 4.2 illustrates how the number of signal and background events change as the program applies more cuts

Cuts	Osc	Beam	CC	NC
None	309	98	1272	3551
Loose	160	15	76	208
ML	81	6	1	5

Table 4.2

The number of events for each type of interaction before the cuts, after loose cuts, and after maximum likelihood cuts.

to the training data set. The program already manages to eliminate a large fraction of the background events, leaving only about 0.2% of the initially generated background events, so any improvements on the FoM would have to be focused on keeping more signal events.

## V. Typical Events

There are three types of events that may occur in the far detector:  $\nu_e$  CC events,  $\nu_\mu$  CC events, and  $\nu_\mu$  NC events. The first are ones that we consider as signal events, while the other two are background events.

$\nu_e$  CC events are characterized by a shower track. This occurs whenever an electron is generated in these events, but is easily distinguishable in quasielastic processes where the events tend to be clean, since the only product of the main interaction is a nucleon and an electron.

Other processes may produce one or multiple  $\pi^0$  that fakes a shower, thus non-quasielastic processes are a bit hard to distinguish from quasi-elastic ones.

In a shower, an electron produces a gamma, which then produces an  $e^+e^-$  pair. The electron from the pair production is then produces another gamma, and the process repeats, creating a track with multiple hits per plane, and scattered hits around the main trajectory. Figure 5.1 illustrates what a typical QE electron event looks like.

$\nu_\mu$  CC events are characterized by a long muon track. Short tracks are also possible when the  $\mu$ -neutrino that initiates the interaction has a low energy, but these events are usually messy and hard to distinguish so that most if not all of the time they get classified as background and eliminated. The main characteristic of a muon track is that it deposits approximately the same amount of energy in every plane, and that they do not shower. So whenever a single track that is found has a uniform energy deposition per plane, it is classified as a muon track and the event gets rejected as a background event. As has been mentioned in the previous section, eliminating  $\nu_\mu$  CC events is rather easy because once a muon track is found to be originated from the main vertex, then that particular event cannot possibly be an electron event, since  $\nu_e$  CC events do not

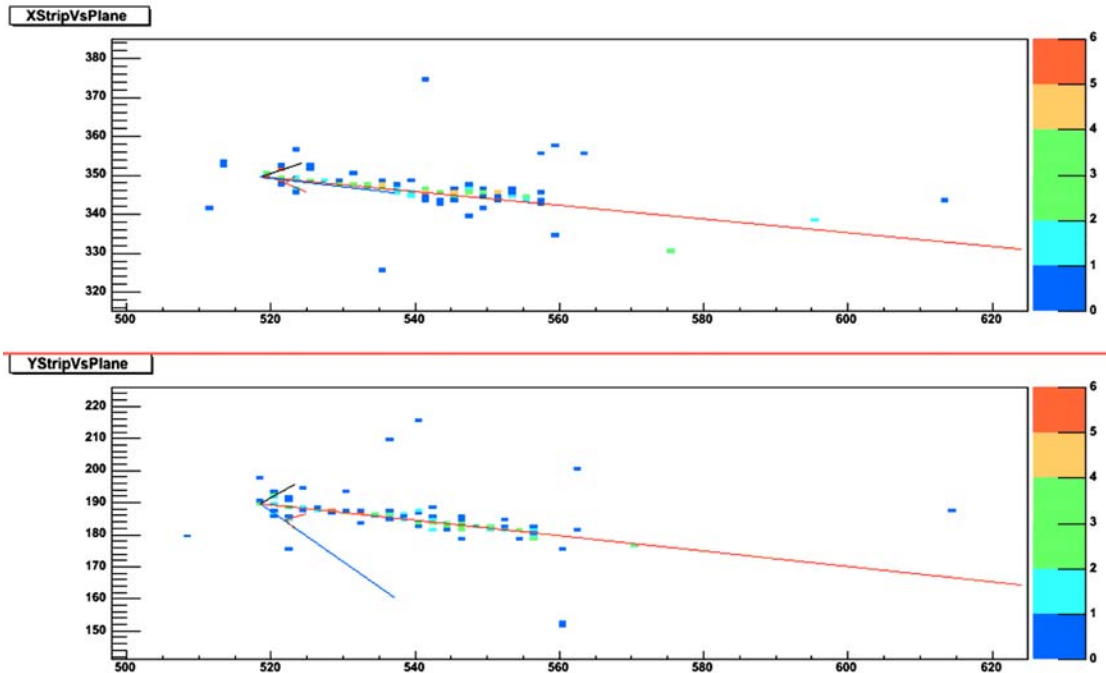


Figure 5.1

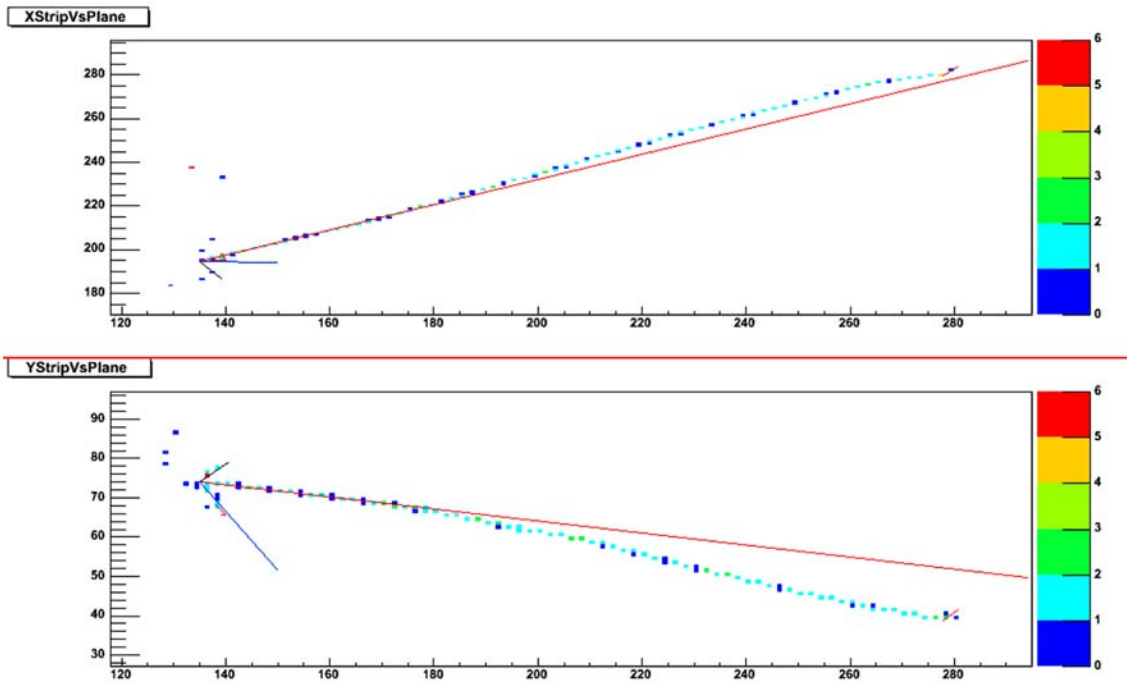


Figure 5.2

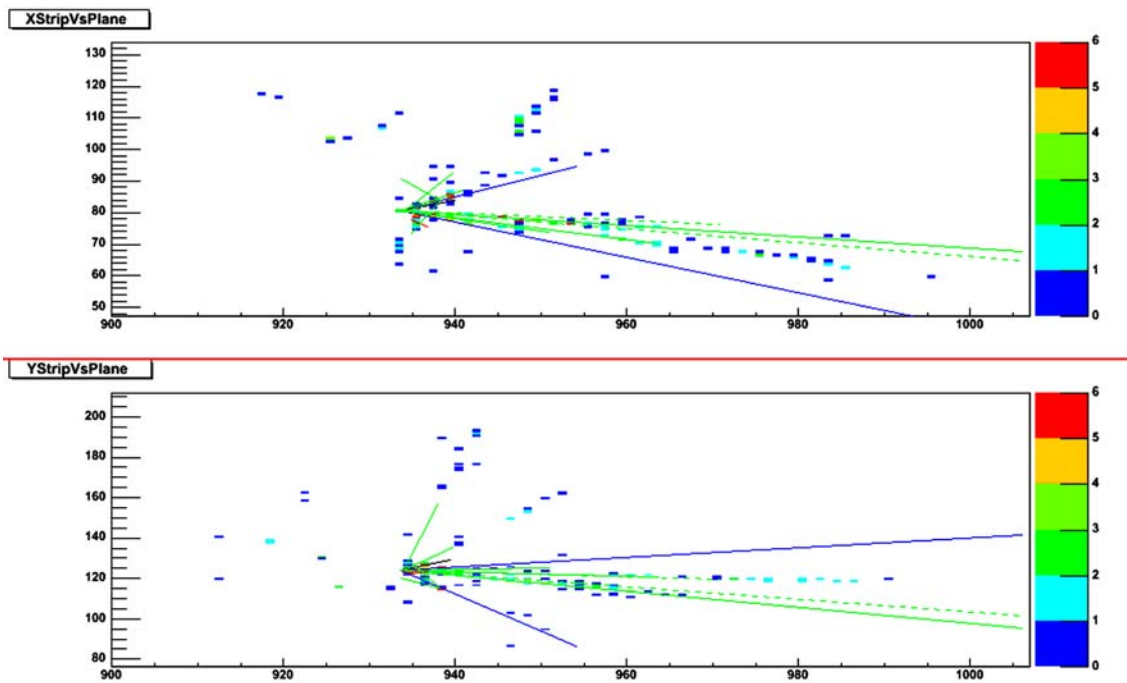


Figure 5.3

produce muons. Figure 5.2 illustrates a typical CC event with a long muon track.

$\nu_\mu$  NC events are characterized by the creation of multiple pions at high energy, and they

tend to be somewhat messy. Charged pions usually create clean single tracks with uniform energy deposition on each plane, but neutral pions may convert to high-energy gammas, which pro-

	Osc	Beam	CC	NC	FoM
Initial	309	98	1272	3551	4.4
+ Loose Cut	160	15	76	208	9.3
ML Analysis	87	7	1	5	23.6
Soft Scan #1	144	12	3	31	21.2
Hard Scan #1	135	9	1	10	30.2
Hard Scan #2	125	8	1	10	28.7

Table 6.1

duces electron-positron pair that creates a showering track. When multiple neutral pions are created, the event tends to look really messy and gets classified as a background event since quasi-elastic electron events are usually clean. Figure 5.3 shows a typical NC event with multiple neutral and charged pions created, along with a few gammas. A feature that distinguishes these showers from the ones initiated by  $\nu_e$  is the gap in front of the shower track. Neutral pions are short-lived, so they decay immediately into gamma rays at the main vertex. Some gamma rays may shower immediately, but some may also travel a certain distance before they finally pair-produce and shower. When the latter happens, there will be no hit on the planes located between the main interaction vertex and the beginning of the shower track because gammas do not deposit energy in the detector. This gap in

front of main vertex is one characteristic to look at when trying to distinguish electron-initiated showers from  $\pi^0$ -initiated showers. Events with gammas that shower immediately have almost no hope of being separated from actual signal events. Figure 5.4 shows a  $\nu_\mu$  NC process that successfully fakes an electron event and survives the maximum likelihood cut.

## VI. Scanning Result

To determine how much more the program can be improved, the result given by the program is compared with the result from actual scanning done by the author.

The procedure is simply for a person to scan the events that pass the loose cuts from a generated typical experiment with a five-year exposure and determine whether an event can be accepted as being an oscillation event or not. The accepted events are then compared to the truth, to see how many of them actually came from  $\nu_e$  interactions. The ones that did are called “signal,” and the ones that did not are called “background.” From here, the FoM can be calculated. Table 6.1 shows the result of the soft scanning—where both possible and probable electron events

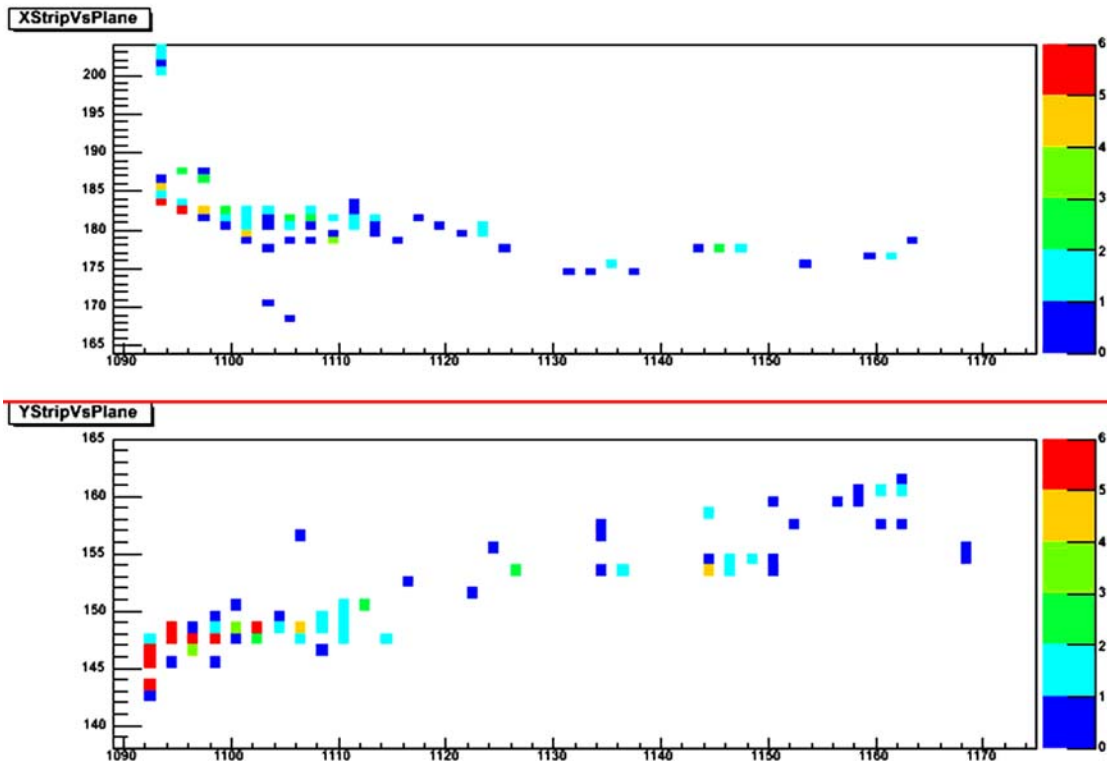


Figure 5.4

are kept—and hard scanning—where only the probable ones are kept and the possible ones are thrown away—in comparison to the program’s maximum likelihood analysis applied to the same set of data. The data used to obtain this result is a different set of data from the one used to obtain the result in table 4.2. The data set used in table 4.2 is one half of the generated data, for the purpose of obtaining the cutoff value that maximizes the FoM of that set. This cutoff value is then applied to the other half of the generated data to give the ML Analysis result seen in table 6.1.

As seen from the table, soft-scanning results in a lower FoM than that of the program, while hard-scanning gives a higher FoM. Although they do not differ by much and is approximately still of the same order, this shows that the event selection program can be further improved.

The table also shows that the program eliminates quite a lot of the signal events, which was mentioned earlier as being somewhat concerning. The program manages to eliminate more background events than the scanner, but the scanner manages to keep more signal events, which results in a higher FoM.

To understand why the program eliminates almost half of the signal events that have passed the loose cuts, further examinations are done on the signal events that did not survive the maximum likelihood cut, but got selected by the scanner. Events that look like a perfectly fine long electron shower are the ones with total likelihood value bordering 6.25, and therefore did not get selected simply because of statistical issues. There are other events, however, that have a negative total likelihood value, but got selected by the scanner. Most of these events display one or more of the following characteristics:

1. Short shower track
2. Multiple hits behind the main vertex
3. One or more  $\pi^0$  produced in the main interaction

Characteristics (1) and/or (3) usually occur in messy events, and it is therefore rather hard to distinguish the electron shower track using only numerical characteristics. These events managed to get selected by the scanner because they survived the following tests:

- No long muon track
- No gap in between the main vertex and a shower track

- Shower tracks have the same length in both views
- Random, scattered hits at the end of the shower track
- If there are gaps on the shower track, each segment has to have the same length in both views.
- Shower pulse height profile is similar in both views
- The individual hits in the shower have a random variation in pulse height.

Characteristics (2) occurs in many clean events which should have passed the maximum likelihood cut, but have negative total likelihood values instead and ended up being rejected as background events. It is possible that these backwards hits caused the reconstruction program to have calculated the location of the main interaction vertex incorrectly. Since the ntuples do not contain information about the vertex position, it was not possible in the time available to also check the reconstruction program.

Figure 6.1-6.5 provide examples of events that exhibit one or more of the three characteristics discussed above.

## VII. Conclusion

Since the events analyzed using maximum likelihood analysis and scanning are all the ones that have passed the loose numerical cuts, there is little to be done in terms of redefining these cuts. The three parameters mentioned in section

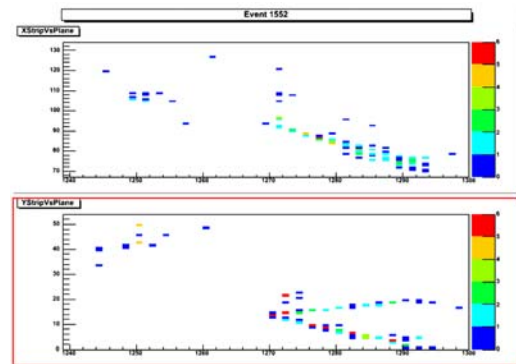


Figure 6.1

X and Y view of an electron event with negative total likelihood. X-view shows clear shower, which is justified by Y-view. Although there are hits on the edge of the detector, the amount of energy deposition is not significant. This event passed the seven tests listed above, but failed the maximum likelihood analysis. It is therefore likely that the reconstruction program failed to find the correct main vertex due to the multiple hits behind the actual main vertex.

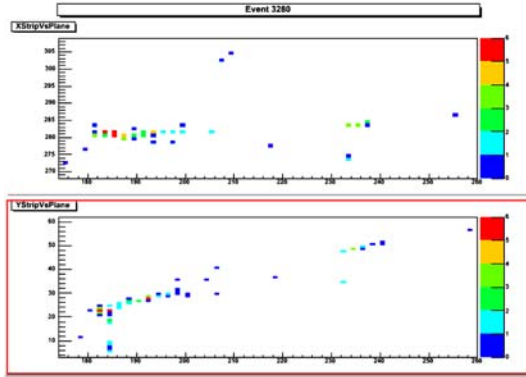


Figure 6.2

Two segments of a shower track are shown in both views to have random variation of pulse heights and si-milar lengths. There are a couple of backwards hits, but the problem in finding the main vertex is most likely caused by the unclear track of the proton produced from the coherent process.

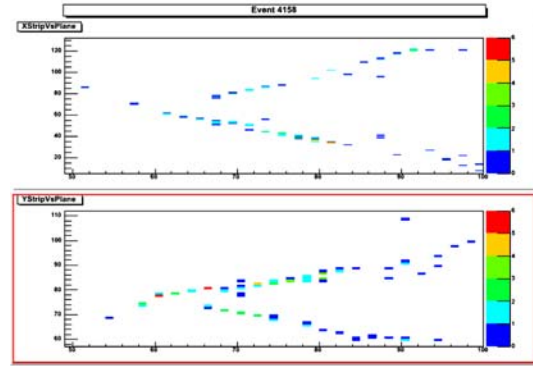


Figure 6.3

This resonant process produces an electron, a neutral pion, and a proton. The proton has a low kinetic energy and thus is unable to go very far. The reconstruction program is most likely having problem in finding the main interaction vertex for this event due to the multiple backwards hits and the gap in the gamma track. The shower track with no gap at the vertex, however, can be claimed to be an electron shower due to the random scattered hits at the end of the track.

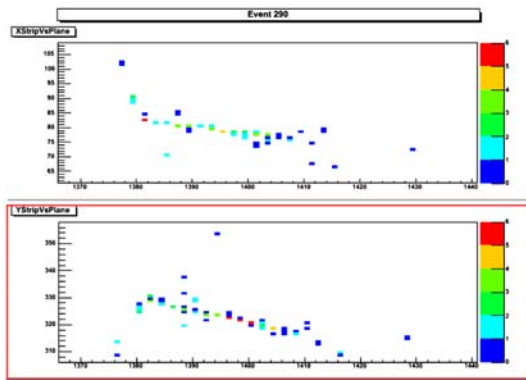


Figure 6.4

This event exhibits the characteristics of an electron shower, with random pulse height variation in the individual hits in the shower, and scattered random hits at the end of the shower track. It failed to pass the ML analysis and has a negative total likelihood value, most likely because of the multiple backwards hit.

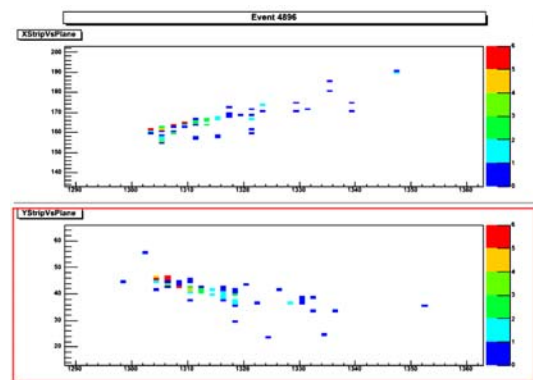


Figure 6.5

Interaction from a Resonant process. Both views show a nice showering track, with similar profile, length, random variation in pulse height, and low-energy randomly scattered hits at the end of the track, but this event has a total likelihood of -5. There are a few backwards hits that might have caused the reconstruction program to have calculated the wrong vertex.

IV (unused PH fraction, no. of gaps, and PH fraction in the first 50% of the planes) proved to be ineffective in the maximum likelihood analysis of this program, and should either be excluded entirely, or studied further to improve the separation of signal from background for these parameters. The event selection program's maximum likelihood analysis has done the best it could, and therefore further improvement should be focused on the reconstruction program, mainly to eliminate characteristic (2) in section VI.

## VIII. References

- 1 – The NOvA Collaboration, *NOvA Proposal*, March 2005
- 2 – D.H. Perkins, *Introduction to High Energy Physics, 4<sup>th</sup> Edition*. Cambridge University Press, 2000.
- 3 – ROOT User's Guide, <http://root.cern.ch/root/doc/RootDoc.html>
- 4 – MINOS Offline Software User's Manual, [http://www-numi.fnal.gov/offline\\_software/srt\\_public\\_context/WebDocs/WebDocs.html](http://www-numi.fnal.gov/offline_software/srt_public_context/WebDocs/WebDocs.html)

## IX. Acknowledgements

I would like to express my utmost gratitude to my project advisor, Professor Peter Litchfield for all the help and guidance throughout the program, Professor Daniel Cronin-Hennessy for all the helpful insights, and the graduate students in the office: Bernard Becker, Jeremy Gogos, Benjamin Speakman, and Dipu Rahman for all the coding hints, error-message handling, and the brief historical background of MINOS and the Greeks. Also included in the list are Serge Rudaz, Maureen Long, and the University of Minnesota for organizing the program, the seminars, the GRE prep courses, the demonstrations, and particularly, the delicious lunches. Last but certainly not least, the utmost gratitude also extends to the National Science Foundation, grant NSF/PHY-0139099, without which this program could not have been made possible.